HHS Public Access

Author manuscript

J Bone Miner Res. Author manuscript; available in PMC 2017 February 01.

Published in final edited form as:

J Bone Miner Res. 2016 February ; 31(2): 430–442. doi:10.1002/jbmr.2690.

Isolation and functional analysis of an immortalized murine cementocyte cell line, IDG-CM6

Ning Zhao[#1,4], **Francisco H. Nociti Jr**[#2,3], **Peipei Duan**[1,6], **Matthew Prideaux**[1,5], **Hong Zhao**[1], **Brian L. Foster**[2,7], **Martha J. Somerman**[2], and **Lynda F. Bonewald**[1]

[1]Department of Oral and Craniofacial Sciences, School of Dentistry, University of Missouri-Kansas City, Kansas City, MO, USA

[2]Laboratory of Oral Connective Tissue Biology, National Institute of Arthritis and Musculoskeletal and Skin Diseases (NIAMS), National Institutes of Health (NIH), Bethesda, MD, USA

[3]Department of Prosthodontics and Periodontics, Division of Periodontics, School of Dentistry at Piracicaba, Piracicaba, Sao Paulo, Brazil

[4]Department of Orthodontics, Shanghai Key Laboratory of Stomatology, Shanghai No. 9 Hospital, Shanghai Jiaotong University School of Medicine, Shanghai, China

[5]Bone Cell Biology Group, Centre for Orthopaedic & Trauma Research, University of Adelaide, Adelaide, Australia

[6]Department of Orthodontics, State Key Laboratory of Oral Diseases, West China College of Stomatology, Sichuan University, Chengdu, China

[7]Division of Biosciences, College of Dentistry, The Ohio State University, Columbus, OH, USA

[#] These authors contributed equally to this work.

Abstract

The dental cementum covering the tooth root is similar to bone in several respects, but remains poorly understood in terms of development and differentiation of cementoblasts, as well as the potential function(s) of cementocytes residing in the cellular cementum. It is not known if the cementocyte is a dynamic actor in cementum metabolism, comparable to the osteocyte in the bone. Cementocytes exhibit irregular spacing and lacunar shape, with fewer canalicular connections compared to osteocytes. Immunohistochemistry and quantitative PCR (qPCR) revealed that the *in vivo* expression profile of cementocytes paralleled that of osteocytes, including expression of dentin matrix protein 1 (*Dmp1*/DMP1), *Sost*/sclerostin, E11/gp38/podoplanin, *Tnfrsf11b* (osteoprotegerin; OPG), and *Tnfsf11* (receptor activator of NF-kB ligand; RANKL). We used the Immortomouse$^{+/-}$; *Dmp1*-GFP$^{+/-}$ mice to isolate cementocytes as *Dmp1*-expressing cells followed by immortalization using the interferon (IFN)-γ-inducible promoter driving expression of a thermolabile large T antigen to create the first immortalized line of cementocytes, IDG-CM6. This cell line reproduced the expression profile of cementocytes observed *in vivo*, including alkaline phosphatase activity and mineralization. IDG-CM6 cells expressed higher levels of *Tnfrsf11b*, and lower levels of *Tnfsf11* compared to IDG-SW3 osteocytes, and under fluid flow

Address correspondence to: Lynda F Bonewald, PhD, 650 East 25th Street, Kansas City, MO 64108, USA, bonewaldl@umkc.edu.

shear stress, IDG-CM6 cells significantly increased OPG while decreasing RANKL, leading to a significantly increased OPG/RANKL ratio, which would inhibit osteoclast activation. These studies indicate similarities yet potentially important differences in the function of cementocytes as compared to osteocytes and support cementocytes as mechanically responsive cells.

INTRODUCTION

Dental cementum, a mineralized tissue covering the tooth root dentin, is present in two types, acellular and cellular [1]. Acellular cementum covers the cervical tooth root and is critical for tooth attachment to the periodontal ligament. Cellular cementum covers the apical root and plays a role in tooth movement and adaptation to occlusion. Cementum resembles bone in several respects, including extracellular matrix composition and mineralization, however, unlike bone, cementum is avascular, non-innervated, and does not undergo physiological remodeling, but grows and is repaired by apposition. Cementum formation can be inhibited by genetic disorders [2], or lost due to tooth root resorption, and periodontal diseases, affecting 47% of U.S. adults, and 70% of those 65 years or older [3]. Absent or defective cementum results in periodontal breakdown, tooth dysfunction and loss. While cementum can be regenerated, current therapeutic strategies are limited and outcomes remain unpredictable [4].

A significant barrier to improved therapies for regeneration is that cementum remains poorly understood. Fundamental questions centering on cementocytes include whether they are physiologically active cells, whether they remain in communication with cells in the PDL region, whether they are involved in cementum formation and repair, including response of cementum to altered demands of tooth use, and whether they regulate osteoclast activity at the cementum surface.

Previously thought to be passive cells residing within the bone matrix, osteocytes are now recognized as the predominant cells modulating bone homeostasis and remodeling, acting as mechanical sensors, and participating in endocrine regulation of mineral metabolism [5-7]. This paradigm shift is the result of more than two decades of intense study of osteocytes *in vivo* and *in vitro*. Here we asked whether the cementocyte is a dynamic actor in cementum comparable to the osteocyte in the skeleton, responding to local stimuli and endocrine signals, and directing local cementum metabolism. We examined cementocytes and their dendritic processes and lacunar-canalicular network ex *vivo*, analyzed the expression profile of freshly harvested cementocytes, used a novel approach to isolate and characterize the first immortalized line of cementocytes, and analyzed effects of shear stress on the cementocyte transcriptional profile. We used osteocytes as a logical comparison because they are most closely aligned to cementocytes as terminally differentiated cells residing in a mineralized matrix.

MATERIALS AND METHODS

Animals

Animal experiments were approved by the Institutional Animal Care and Use Committee (IACUC) of the University of Missouri at Kansas City (UMKC), and the Animal Care and Use Committee (ACUC) of the National Institute of Arthritis and Musculoskeletal and Skin Diseases (NIAMS) of the National Institutes of Health (Bethesda, MD, USA), in accordance with federal regulations. For histology, scanning electron microscopy, and analysis of cell-specific gene expression in bones and teeth, 2-3 month old male C57BL/6 mice were used for tissue harvest. For isolation of cementocyte cell lines, the Immortomouse was crossed with the *Dmp1*-GFP mouse (Immortomouse$^{+/-}$/*Dmp1*-GFP$^{+/-}$ mouse), as described previously for generation of the IDG-SW3 late osteoblast/early and late osteocyte cell line [8]. All mice were housed in standard conditions of temperature (23 ± 2°C) in a light-controlled environment, with unlimited access to water and pelleted food (UAR rodent diet No.R03-25; UAR, Epinay/Orge).

Histology

Tissues were harvested and fixed in 10% formalin for 24 hrs followed by decalcification in 14% EDTA (pH 7.1) and embedded in paraffin. 5 μm thick serial sections were cut and stained with hematoxylin and eosin (H&E) for light microscopy.

For immunohistochemistry, deparaffinized tissue sections were treated with primary antibodies (detailed below), biotinylated secondary antibodies, with localization detected using a peroxidase kit (Vector Labs, Burlingame, CA), and 3, 3'-diaminobenzidine (DAB) substrate (Sigma, St. Louis, MO) or 3-amino-9-ethylcarbazole (AEC) substrate (Vector Labs), and counterstained with 0.5% methyl green or Harris' hematoxylin. Non-immune IgG/serum was used in lieu of primary antibody as a negative control. Primary antibodies included polyclonal rabbit IgG anti-dentin matrix protein 1 (DMP1 at 1:600 dilution; Takara Bio, Shiga, Japan), polyclonal goat IgG anti-sclerostin (SOST at 1:100 dilution; R&D Systems, Minneapolis, MN), monoclonal hamster IgG anti-E11 8.1.1 (1:100 dilution), polyclonal rabbit IgG anti-DSP LF-153 (1:200 dilution), and monoclonal rabbit IgG anti-THY1/CD90 (1:50 dilution; Abcam, Cambridge, MA).

For fluorescein isothiocyanate labeling, mandibles were fixed in 4% paraformaldehyde at 4°C with gentle shaking for 24 hrs, then transferred to 70% ethanol for 24 hrs before embedding using Sampl-Kwick Fast Cure Acrylic kit (Buehler, Lake Bluff, IL). A diamond saw was used to cut 150-300 μm sections that were ground down to 70-100 μm using graded sand paper. Specimens were dehydrated in a graded ethanol series, then stained in 1% fluorescein isothiocyanate for 4 hrs at room temperature, followed by 100% ethanol wash for 30 min. Samples were air dried for 2 hrs before mounting for confocal microscopy.

Scanning election microscopy (SEM)

Mandibles were embedded in methylmethacryate and polished with successively finer particle size diamond suspensions until smooth. For SEM cultured cells were washed with PBS and fixed with 10% formalin for 20 min, rinsed with PBS, dehydrated in a graded

ethanol series, and dried using hexamethyl disilazone for 5 min. Coverslips were attached to a stub and sputter coated with gold palladium. FEI/Philips XL30 Field emission environmental SEM in backscatter mode was used, as described previously [8, 9].

For SEM of acid-etched samples, surfaces of polished resin-embedded samples were treated with 37% phosphoric acid for 2-10 sec, rinsed with water, immersed in 5% sodium hypochlorite for 5 min, and rinsed in water. After air drying, samples were coated with gold and palladium and examined by FEI/Philips XL30 Field emission environmental SEM, as described previously [9].

Isolation of primary tissue-specific mRNA

In order to quantitatively compare "*in situ*" gene expression of cementocytes to other dental and bone cells, primary cells were harvested from 3 month old male C57BL/6 mice. Tissues isolated included cellular cementum, molar pulp, incisor pulp, alveolar bone, and long bone (n=4 each). Osteocytes were enriched from long bones by serial enzymatic digestion as described previously [10]. For isolation of osteocytes from alveolar bone, the same digestion protocol applied to dissected alveolus. Cementocytes were enriched from first mandibular molar cellular cementum using the same enzymatic digestion approach, with a dissecting microscope employed to remove the apical root tip following the last step of enzymatic digest. For isolation of incisor pulp, mandibular incisors were dissected and transferred to α-MEM with 1% penicillin and streptomycin, and dentin was dissected to expose the dental pulp for collection. For isolation of molar pulp, the molar crown was dissected from the tooth root to expose the pulp complex within. Isolated cell populations were placed into 1 ml TRIzol Reagent (Life Technologies, Carlsbad, CA) and stored at −80°C until total RNA was isolated for cDNA synthesis and real-time quantitative polymerase chain reaction.

Cementocyte isolation and cloning

Steps in the procedure for enzymatic isolation of cementocytes are outlined in Table 1. Cell culture reagents including alpha-MEM media, antibiotics, Hanks balanced salt solution (HBSS), and trypsin-EDTA, were purchased from Mediatech, Inc. (Manassas, VA). Mandibles were harvested from 3-month-old Immortomouse$^{+/-}$/*Dmp1*-GFP$^{+/-}$ female mice (n=4). These mice carry an interferon (IFN)-γ-inducible promoter driving expression of a thermolabile large T antigen (H-2Kb-tsA58), enabling conditional immortalization of cells derived from their tissues [11]. Genotypes were verified by GFP expression in tail biopsies and by PCR analysis of genomic DNA, as described previously [12]. Mandibles were rinsed in 70% ethanol and immersed in alpha-MEM media containing 1% Pen/Strep antibiotics and gentamycin (250 μg/mL) at room temperature until tooth extraction (completed within 30 min). A dissecting microscope and scalpel were used to extract first to third mandibular molars, as described previously [13]. Apical portions of tooth roots were detached with a scalpel and used for isolation of cementocytes from cellular cementum. Periodontal ligament and pulp tissues were removed from cementum by enzymatic digestion with 300 U/mL type I collagenase (Sigma) for 30 min at 37°C, then the supernatant was discarded. Cellular cementum fragments were subjected to serial digestion with 3 cycles of collagenase A (300 U/mL) and EDTA (5 mM, in 0.1% bovine serum albumin; BSA) for 20 min each at 37°C, in order to allow cementocyte migration from the cementum matrix. Root fragments were

rinsed in HBSS and incubated in 37°C on collagen coated plates with alpha-MEM containing 10% fetal bovine serum (FBS), 1% Pen/Strep, and gentamycin (250 μg/mL), without IFN-γ. 48 hrs later, cementum fragments were transferred to media containing IFN-γ (50 U/mL; Life Technologies) and incubated at 33°C.

At 96 hrs, roots were cut into smaller fragments for cells to migrate to the culture surface and cultured for an additional week in growth media containing 50 U/mL IFN-γ, with media changed every 3 days in order to obtain sufficient numbers of cells for freezing cell stocks and single cell cloning.

To produce clonal populations, serial dilutions of isolated cementocytes in suspension were performed to achieve an average of a single cell per well in 96-well plates. Wells containing a single cell were selected for expansion and maintained in growth media with 50 U/mL IFN-γ at 33°C. After reaching 40% confluence, cells were released from dishes with 0.05% trypsin EDTA and transferred to larger plates to prepare frozen stocks and perform experiments.

Cell culture experiments

In order to analyze the cementocyte phenotype, clones of immortalized cementocytes were compared to IDG-SW3 cells, an immortalized osteocyte-like cell line isolated from the same Immortomouse$^{+/-}$/*Dmp1*-GFP$^{+/-}$ mice [8]. Cementocytes and osteocytes were plated and treated under the same conditions for all experiments. Cells were plated in growth media at 33°C at an initial density of 4×10^4 cells/cm^2. After reaching 100% confluence in 2 days, growth media were replaced with differentiation media containing 50 μg/ml ascorbic acid and 4 mM β-glycerophosphate, without INF-γ, and cells were cultured at 37°C. The green fluorescent signal generated by the *Dmp1*-GFP was confirmed every 3 days (see below). After selection of positive clones, cell culture conditions and testing were performed as described previously for IDG-SW3 cell culture, except where otherwise noted [8].

For quantification of GFP expression in cementocytes, 15 μl of cell lysate was measured in a Victor II fluorescent plate reader. Relative fluorescent units (RFU) were normalized to total protein concentration, measured using BCA assay (Thermo Fisher Scientific, Rockford, IL), as described previously [8].

Fluid flow shear stress (FFSS) was applied to cells in order to analyze transcriptional response to mechanical stress, an approach previously used for MLO-Y4 osteocytes [14-16]. Cells were plated onto slides for 21 days before being tested in a Streamer Gold apparatus at 2 dynes/cm^2 for 2 hrs. After 2 hrs, total RNA was harvested for gene expression analysis (see below).

Alkaline phosphatase (ALP) activity assay, *in vitro*

Cells were lysed with 0.05 % Triton-X and two freeze-thaw cycles. ALP activity was assayed with 1.5 M 2-amino-2-methyl-1-propanol buffer (pH 10.3) and quantified using a p-nitrophenol phosphate standard curve, as described previously [17]. Absorbance at 405 nm was recorded in triplicate and normalized to total protein levels determined by BCA assay.

Mineralization assay, *in vitro*

Alizarin red staining and quantitation were used to measure mineralization capacity. Cells were fixed in 10 % neutral buffered formalin for 10 min at 4 °C and then stained with 2% w/v alizarin red-S solution at pH 4.2 for 5 min. After removal of dye and rinsing several times in phosphate buffered saline (PBS) to remove unbound dye, images were taken. To quantify calcium deposition, dye was eluted from the monolayer by addition of 1 ml 10% cetylpyridinium chloride solution. 200 μl was transferred to a 96-well plate, and optical density measured at 570 nm.

Western blot

To measure protein expression, cell monolayers were scraped from dishes and placed in RIPA buffer containing protease inhibitors (Sigma) as described previously [18]. 10 μg of total protein was loaded onto a 10% Bis-tris gel (Bio-Rad Laboratories, Hercules, CA) and separated by SDS PAGE electrophoresis. Protein bands were detected using the SuperSignal West Dura Chemiluminescence kit (Pierce). Densitometry was performed using Multi-Gauge software (Fujifilm Corporation, Tokyo, Japan). Primary antibodies for Western blot were the same as for immunohistochemistry (described above). The anti-sclerostin antibody was used at 1:500 and anti-E11 at 1:2500.

Real-time quantitative polymerase chain reaction (qPCR)

To measure gene expression in cells enriched from primary tissue or cells *in vitro,* total RNA was isolated using TRIzol reagent according to manufacturer's instructions (Life Technologies). 1 μg mRNA was reverse transcribed to cDNA (High-capacity cDNA reverse transcription kit, Life Technologies). Real-time PCR was conducted using TaqMan Gene Expression Mix and gene-specific TaqMan probes (Applied Biosystems, Foster City, CA). The $2^{-\Delta\Delta C_T}$ method was used to analyze the relative gene expression and normalized to b-actin. The fold changes were calculated and shown in each figure along with the C_t value. C_t is the intersection between amplification concentration and threshold and is a relative measure of concentration of the target mRNA.

Statistical analysis

Statistical analyses were performed by Student's t-test, one-way ANOVA followed by Tukey post-hoc test, or two-way ANOVA followed by Tukey post-hoc test (for intragroup) or Bonferroni post hoc test (for intergroup) to determine significant differences (GraphPad Prism 6.0). Statistical significance was indicated by p-value < 0.05. Quantitative data are reported as mean ± standard deviation (SD) for one representative experiment (performed in triplicate; n=3) out of three or more experiments, unless otherwise stated.

RESULTS

Differences in lacunar-canalicular network of cementocytes compared to osteocytes

As a first step to analyze cementocytes *in situ*, we performed a morphological analysis of the lacunar-canalicular network in cellular cementum of a mouse first mandibular molar (Figure 1A). In addition to expected observations of single cementocytes occupying lacunae,

histology revealed numerous empty cementocyte lacunae (data not shown) and lacunae containing multiple cells (Figure 1B), never observed for osteocytes in alveolar bone (Figure 1C) or other regions of cortical bone. Backscatter SEM revealed that, compared to regular spacing and ellipsoid shape of osteocyte lacunae, cementocyte lacunae were irregularly shaped and unevenly distributed in the matrix (Figure 1D-H). SEM examination of acid etched resin-embedded mandibles revealed numerous canaliculi of osteocytes, whereas cementocytes exhibited large, irregular lacunae with fewer canaliculi (Figure 1I-L), observations confirmed by FITC staining (Figure 1M, N).

Generation of DMP1-positive cementocyte cell line, IDG-CM6

Differences in cementocyte dendrites, lacunar shape, and canalicular networks compared to osteocytes (Figure 1) suggested functional differences in these cells, *in vivo*. To define properties of cementocytes, and identify similarities and differences to osteocytes, we isolated, cloned, and performed a functional analysis of an immortalized cementocyte cell line. To distinguish cementocytes from surrounding cells, we utilized the fact that cementocytes express dentin matrix protein (DMP1) [Figure 1A, B and [19]]. Use of Immortomouse$^{+/-}$; *Dmp1*-GFP$^{+/-}$ mice allowed identification of *Dmp1*-expressing cells and immortalization via interferon (IFN)-γ-inducible promoter driving expression of a thermolabile large T antigen [11], similar to the approach used to generate osteocyte-like cell line IDG-SW3 [8].

For isolation of cementocytes from surrounding cells, molars were extracted to exclude alveolar bone, and the apical portion of the molar root (including cellular cementum) was dissected (Figure 2A). DMP1-GFP expressing cells in the apical tooth included cementocytes and odontoblasts (Figure 2B). During enzymatic digestion to release cementocytes from the cementum matrix (Table 1), GFP-positive cells were tracked from within the digested matrix to migration onto the culture dish (Figure 2C).

Serial dilution of the isolated cells resulted in over 1,500 colonies, and more than 30 single-cell clones were obtained. Out of 17 GFP-positive single cell clones, 2 clonal cell lines were profiled further, and the IDG-CM6 line was selected for studies described here. These cells were isolated from female mice and the gender confirmed by PCR analysis (data not shown). After 30 days in culture, IDG-CM6 cells maintained a high GFP signal and exhibited the characteristic dendritic cementocyte morphology (Figure 2D). Furthermore, SEM analysis of IDG-CM6 cells after 14 days in culture confirmed production of an extracellular matrix of collagen (Figure 2E).

Dmp1 gene expression was analyzed in cementocytes *in vivo* and *in vitro*. qPCR analysis of isolated tissues indicated *Dmp1* was expressed in cellular cementum as well as in long bone, alveolar bone, and molar and incisor dentin-pulp complex (Figure 2F), validating this marker for selective isolation of cementocytes. *Dmp1* and *Col1a1* gene expression profiles over 42 days were similar between IDG-CM6 cementocytes and IDG-SW3 osteocytes (Figure 2G-J).

IDG-CM6 cementocytes mineralize in culture

The capability to promote deposition of hydroxyapatite mineral *in vitro* is one marker for mineralizing cells. IDG-CM6 were cultured under mineralizing conditions (50 μg/ml ascorbic acid, 4 mM β-glycerophosphate) and compared to IDG-SW3 osteocytes. A similar profile in GFP expression was observed in IDG-CM6 and IDG-SW3, however, cementocytes were slower to achieve peak GFP signal (day 35 vs. day 21 in IDG-SW3 cells) (Figure 3A, C). By alizarin red staining, increased mineral deposition by IDG-CM6 was observed by day 7, whereas IDG-SW3 cells initiated mineralization by day 14 (Figure 3B, D), similar to previous results [8]. Both cell lines became highly mineralized over 42 days. ALP activity increased in both cells over days 3-14 (Figure 3E), coincident with increased mineral deposition. IDG-SW3 cells showed relatively less ALP activity by days 14-28.

IDG-CM6 cementocytes express sclerostin and E11/gp38

Sclerostin, a marker for mature osteocytes, is a regulator of osteoblast function and bone formation [5, 20]. Sclerostin localization has been reported in human and mouse cementocytes [21-23] and *Sost*$^{-/-}$ mice feature alterations in cellular cementum [24].

We confirmed sclerostin immunolocalization in mouse cementocytes and alveolar bone osteocytes, concentrated in the lacunar regions (Figure 4A, B). Sclerostin was not identified in dental pulp or odontoblasts. qPCR from tissues confirmed expression of *Sost* mRNA in bone and cementum, and barely detectable levels in molar and incisor pulp (Figure 4C). Lower expression of *Sost* in pulp vs. cementum supports that IDG-CM6 cells are not derived from dental pulp, a potential contamination of the isolated cementum.

When cultured under mineralizing conditions, IDG-CM6 expressed robust levels of *Sost* mRNA and sclerostin protein, in a biphasic profile with peaks at days 14 and 42 (Figure 4D, F). In contrast, IDG-SW3 cells expressed lower levels of both *Sost* mRNA and sclerostin protein compared to IDG-CM6 cells, and expression was not detected until day 21 (Figure 4E, G).

E11/gp38/podoplanin, an early osteocyte-selective protein, is thought to play a role in formation of dendritic processes [25, 26]. E11 protein was identified in rat cementocytes [27], as well as odontoblasts [28]. Immunostaining showed high E11 expression in tibia especially in newly embedded osteocytes, with less intensity in alveolar bone and cellular cementum (Figure 5A-C). qPCR confirmed expression of *E11/gp38* mRNA in isolated bone and cementum, and in dental pulp (Figure 5D). Both IDG-CM6 and IDG-SW3 expressed *E11/gp38* mRNA and protein over the course of 3-42 days in mineralizing conditions *in vitro,* with peak expression at early stages, days 7-14 (Figure 5E-H).

The dentin sialophosphoprotein (*Dspp*) gene, and associated proteins dentin sialoprotein (DSP) and dentin phosphoprotein (DPP), initially identified in odontoblasts and dentin matrix, have since been localized to alveolar bone and cellular cementum [29, 30]. DSP immunolocalization in mouse dentoalveolar tissues was limited to dentin and pulp tissues, limited regions of cellular cementum, and some apical alveolar bone (Supplemental Figure 1A-C). qPCR showed *Dspp* expression in pulp of molars and incisors, with little expression in cementum and bone (Supplemental Figure 1D). In cell culture, *Dspp* mRNA was not

detectable/very low in both IDG-CM6 and IDG-SW3 cells consistent with immunostaining and qPCR results (Supplemental Figure 1E-F).

T-cell marker, thymus cell antigen 1 (*Thy1*/THY1), has been used as a marker of dental pulp-derived cells [31], with expression varying by differentiation state, with higher levels found in progenitor cells. By immunohistochemistry, THY1 was not detectable in cementocytes, though it was present in molar and incisor dental pulp (Supplemental Figure 1G-I). qPCR showed *Thy1* mRNA in all tissues, including cementum (Supplemental Figure 1J). In culture, *Thy1* mRNA was very low at all-time points up to 42 days in both IDG-CM6 and IDG-SW3 cells (Supplemental Figure 1K-L).

The levels of osteocalcin (*Bglap*) mRNA were also determined with no significant differences observed between IDG-SW3 and IDG-CM6 cells in expression, nor any changes with differentiation over time in culture. As both cell lines express high levels of *Bglap* mRNA, this suggests the cell lines begin as late osteoblasts and late cementocytes. (Supplemental Figure 2).

IDG-CM6 cells express RANKL and OPG

Osteocytes regulate osteoclastic bone resorption through expression of the osteoclast activator, receptor activator of nuclear factor kappa-B ligand (RANKL), and the inhibitor of osteoclastogenesis, osteoprotegerin (OPG), as well as other factors [7, 32-35]. While cementoblasts express RANKL and OPG [36], it has remained unreported whether cementocytes express RANKL or OPG, and if the cells play a parallel role to osteocytes in controlling osteoclast activation around the tooth root.

A comparison of *Tnfrsf11b* (OPG) and *Tnfsf11* (RANKL) mRNA levels in primary tissues from long bone, alveolar bone, and cellular cementum, revealed relatively high *Tnfrsf11b* in cementum, relatively low *Tnfsf11*, and a significantly higher OPG/RANKL ratio in primary cementocytes compared to osteocytes from long bone or alveolar bone (Figure 6A-C). Over the course of 28 days, IDG-CM6 cells expressed significantly higher levels of *Tnfrsf11b* mRNA at early time points, peaking on day 7 (Figure 6D). In contrast, IDG-SW3 cells expressed considerably higher levels of *Tnfsf11* than IDG-CM6 cells, at all-time points (Figure 6E). This relative difference in *Tnfsf11* results in a significantly higher OPG/RANKL ratio in IDG-CM6 cells at days 3, 7, and 21 (Figure 6F), suggesting that cementocytes do not support osteoclast formation and activation, unlike osteocytes.

IDG-CM6 cells exhibit transcriptional changes in response to fluid flow shear stress

Osteocytes are mechanosensory cells responding to alterations in mechanical loading on bone by changing expression of key regulatory factors directing bone remodeling, including RANKL and OPG [5, 37, 38]. Sclerostin, an inhibitor of canonical *Wnt* signaling, is down-regulated in osteocytes by anabolic stimuli, including mechanical loading [7, 37], and is expressed by cementocytes *in vitro* (Figure 4) and *in vivo* [22, 23]. Fluid flow shear stress (FFSS) has been used to analyze *in vitro* the response of osteocytes to mechanical loading [14, 15, 39], and here was used to determine whether and how IDG-CM6 cementocytes respond to mechanical stimuli.

IDG-CM6 and IDG-SW3 cells were grown for 21 days, then subjected to FFSS for 2 hrs at 8 dynes/cm^2, and mRNA was harvested. *Sost* mRNA was decreased significantly in both cell types by shear stress (Figure 6G). FFSS stimulated a significant 4-fold increase in *Tnfrsf11b* in IDG-CM6 cells, while IDG-SW3 cells showed a non-significant trend in the same direction (Figure 6H). In response to FFSS, IDG-CM6 cells significantly decreased *Tnfsf11*, whereas IDG-SW3 cells showed a significant increase (Figure 6I). Cementocytes exhibited a statistically significant 40-fold increased OPG/RANK ratio, suggesting negative regulation of osteoclastogenesis, while osteocytes show non-significant changes under the same FFSS conditions (Figure 6J).

DISCUSSION

Dental cementum covering the tooth root is similar to bone, but remains poorly understood in several respects, including potential function(s) of the terminally differentiated cementocytes residing in the cellular cementum [1]. Once thought to be passive cells residing within bone, osteocytes are now recognized to actively modulate bone homeostasis and remodeling, respond to mechanical loading, and contribute to endocrine regulation of mineral metabolism [5-7]. It has long been unclear whether the cementocyte is a dynamic actor in cementum metabolism, comparable to the osteocyte in the skeleton. Here, we analyzed cementocytes to better understand the functional properties of these cells, using alveolar and long bone, and immortalized IDG-SW3 osteocytes as logical points of comparison.

Histology and SEM confirmed that cementocytes reside in lacunae and develop a canalicular network, however they exhibit irregular spacing and lacunar shape, and fewer dendritic connections compared to osteocytes. The *in vivo* expression profile of cementocytes paralleled that of osteocytes, including expression of *Dmp1*/DMP1, *Sost*/Sclerostin, *E11/gp38*, *Tnfrsf11b*, and *Tnfsf11*. We used Immortomouse$^{+/-}$; *Dmp1*-GFP$^{+/-}$ mice to create the first immortalized line of cementocytes. One clone selected for detailed analysis, IDG-CM6, reproduced the observed *in vivo* expression profile of cementocytes (including low or no *Dspp* and *Thy1*, indicating lack of pulp/odontoblast contamination), expressed *Col1a1*/collagen and *Alpl*/TNAP and ALP activity, and mineralized *in vitro*. IDG-CM6 cells expressed similar levels of *Tnfrsf11b*, and lower levels of *Tnfsf11* compared to IDG-SW3 osteocytes. In contrast to IDG-SW3 and osteocytes *in vivo*, under FFSS, IDG-CM6 cells significantly increased *Tnfrsf11b* while decreasing *Tnfsf11,* leading to an increased OPG/RANKL ratio that would discourage osteoclast activation (summarized in Figure 6K). Overall, these studies indicate similarities in cementocytes and osteocytes, support cementocytes as physiologically responsive cells, and point to important differences in responses of cementocytes vs. osteocytes to mechanical loading that offer clues about cementum development and maintenance. Moreover, we have established a cell line that can be used to further investigate cementocyte functions in years to come.

Osteocytes reside within a lacuna, their dendritic processes extending through a fluid-filled canalicular network allowing communication and signaling between osteocytes, between osteocytes and surface cells (e.g. osteoblasts, osteoclasts, and others), and between osteocytes and distant cells via endocrine factors [5, 6]. As a first step to understanding the

capabilities of cementocytes, we analyzed their cell morphologies and lacunar-canalicular system using histology and SEM. Cementocytes occupy lacunae and display dendrites within a canalicular network, indicating that they are adapted as cells entombed within a mineralized matrix, capable of communicating with one another and/or cells outside the cellular cementum, i.e. cementoblasts and cells of the PDL space. These observations confirm previous studies on cementocyte networks in rats and humans [40, 41].

However, profound differences were observed between cementocytes and osteocytes, *in vivo*. Cementocyte dendrites are many fewer in number and density, and canalicular networks are not nearly as extensive as those from osteocytes, suggesting less communication between, to, and from cementocytes. This incongruity may reflect fundamental differences in physiology of bone versus cementum. Bone is highly vascular and continuously remodels in response to load, and osteocytes play a central role in orchestrating these processes. On the other hand, cellular cementum is avascular and grows by apposition, with no physiological turnover. In this context, cementocytes are not so densely connected to the vasculature and may not require a high degree of interconnectivity with one another in order to function. An important question is whether cementocytes maintain their connectivity to the surface in order to receive and send signals. Our SEM analyses indicate such connectivity, and previous studies using tracer penetration into extracted human teeth [42] or *in vivo* intravenous injection of tracers into rats [43], provide added support that cementocytes remain connected, even in the deep cementum close to the cementum-dentin junction. Interestingly, cementocytes located farther from the surface are reported to be less metabolically active [43], and over time these cells may lose contact, become quiescent, and die [44]. Our and others' [45, 46] observations of empty cementocyte lacunae support this hypothesis, although additional studies on cementocyte metabolism and cell death are warranted.

We observed that cementocyte lacunae were larger and more irregular in shape than the regular ellipsoid osteocyte lacunae, and that more than one cementocyte was present in some lacunae. Studies on osteoblast to osteocyte transition have provided insights into observed changes in cell shape and polarity, development of dendrites, cell interconnectivity, and adaptations in cell function [summarized in: [5, 6]]. These types of studies on cementoblast-cementocyte transition will reveal much about cementocyte biology.

The IDG-CM6 cell line was characterized to confirm their identity as cementocytes and compare their expression profile to the osteocyte-like IDG-SW3 cell line. IDG-CM6 cementocytes proliferated and promoted mineralization *in vitro*, expressing greater ALP and depositing mineral more rapidly than IDG-SW3 cells. These results confirm previous studies of cementocytes *in vivo* suggesting that these cells participate in secondary calcification of cementoid matrix [40] as proposed for osteocytes in bone [5, 6], and that diseases disturbing biomineralization can result in hypomineralization of cementocyte and osteocyte lacunae and surrounding matrices [2].

Sclerostin/SOST is expressed by mature osteocytes, and negatively regulates bone formation by antagonizing canonical Wnt signaling in osteoblasts. IDG-CM6 cells expressed high levels of *Sost* mRNA and sclerostin protein, in agreement with *in vivo* studies reporting

cementocyte expression [21-23]. Expression of *Sost*/sclerostin by cementocytes suggests that these cells may regulate cementoblast cell activity on the cementum surface. Deletion of *Sost* in mice resulted in increased deposition of cellular cementum, in parallel to more dramatically increased alveolar bone deposition [24] and increased long bone cortical bone and mineral density [47]. Interestingly, IDG-CM6 cells expressed *Sost* mRNA and protein in biphasic fashion, whereas IDG-SW3 osteocytes linearly increased *Sost*/sclerostin in culture.

Osteocytes are mechanosensory cells responsive to changes in bone loading by virtue of their location within bone, their interconnected dendritic processes, and their ability to sense and respond to hydrostatic changes in fluid flow within the lacunar-canalicular system. In response to changes in bone loading, osteocytes can direct osteoblastic and osteoclastic activities at the bone surface to orchestrate bone remodeling [5, 6, 38]. Cementocytes, as cells embedded in cementum and displaying dendrites within canaliculi, may display responsiveness to mechanical stimuli. There are physiological circumstances associated with changes in tooth loading and function where cellular cementum formation is stimulated. For example, cellular cementum begins to form around the time the tooth enters occlusion, and these mechanical forces may have a role inducing the switch from acellular cementum to cellular cementum [44, 48]. Additionally, apposition of cellular cementum is thought to compensate for slow attrition of enamel throughout life, maintaining proper occlusion of teeth. This effect was demonstrated in rodent studies of unopposed super-eruption of teeth, where cellular cementum production was induced [49]. Increased cellular cementum formation was also reported in response to physiological tooth movement in rats, whereas alveolar bone was induced to resorb [50]. Cementum is proposed to have a protective role against osteoclastic resorption, as teeth do not undergo physiological remodeling as bone does, and often resist resorption under conditions where alveolar bone is targeted by osteoclasts (e.g. periodontitis). When cementum is resorbed, cellular “reparative” or “regenerative” cementum is often formed in the course of healing, even on the cervical root [4]. In all these cases, it is unclear whether the cementocyte is an active actor in cementum formation or regulation of local osteoclast function, and why cementum seems resistant to resorption, unlike bone.

We explored this topic by assaying expression of OPG and RANKL *in vivo* and *in vitro*. In fresh tissues, cellular cementum expressed a significantly higher OPG/RANKL ratio than either alveolar or long bone, owing to increased *Tnfrsf11b* and reduced *Tnfsf11*. IDG-CM6 cells also maintained a higher OPG/RANKL ratio than IDG-SW3 cells for most of the 28 day experiment. Interestingly, *in vitro* experiments subjecting cementocytes and osteocytes to FFSS to mimic mechanical stimuli, revealed inherently different cellular responses. Whereas both cell types decreased *Sost* in response to FFSS, IDG-CM6 cells significantly increased *Tnfrsf11b* (no change in IDG-SW3) and significantly reduced *Tnfsf11,* in contrast to increased expression by IDG-SW3 cells. The significantly higher OPG/RANKL in IDG-CM6 cells under stress suggests a potential mechanism for increased cementogenesis and lack of resorption in cellular cementum observed during tooth movement and altered function [49, 50].

In conclusion, the IDG-CM6 cell line should prove useful as a model for future studies for comparison to other cell types such as odontoblasts, for identification of cementocyte markers and for determination and investigation of cementocyte functions,

Supplementary Material

Refer to Web version on PubMed Central for supplementary material.

ACKNOWLEDGMENTS

This work was supported by grant PO1 AR046758 (to LB), by the Intramural Research Program of NIAMS/NIH (to MJS), and by National Natural Science Funds of China (Grant No. 81000420; to NZ). The authors thank Yixia Xie, LeAnn Tiede-Lewis, Vladimir Dusevich, and Jennifer Rosser (University of Missouri-Kansas City, Kansas City, MO) and Alyssa Coulter and K.C. Hemstreet (NIAMS/NIH) for their assistance in these studies.

REFERENCES

1. Foster, BL.; Somerman, MJ. Cementum. In: McCauley, LK.; Somerman, MJ., editors. Mineralized Tissues in Oral and Craniofacial Science: Biological Principles and Clinical Correlates. Wiley-Blackwell; Ames, IA: 2012. p. 169-192.
2. Foster BL, Nociti FH Jr. Somerman MJ. The rachitic tooth. Endocr Rev. 2014; 35(1):1–34. [PubMed: 23939820]
3. Eke PI, et al. Prevalence of periodontitis in adults in the United States: 2009 and 2010. J Dent Res. 2012; 91(10):914–20. [PubMed: 22935673]
4. Bosshardt DD, Sculean A. Does periodontal tissue regeneration really work? Periodontol 2000. 2009; 51:208–19. [PubMed: 19878476]
5. Dallas SL, Prideaux M, Bonewald LF. The Osteocyte: An Endocrine Cell … and More. Endocr Rev. 2013; 34(5):658–690. [PubMed: 23612223]
6. Bonewald LF. The amazing osteocyte. J Bone Miner Res. 2011; 26(2):229–38. [PubMed: 21254230]
7. Bellido T. Osteocyte-driven bone remodeling. Calcif Tissue Int. 2014; 94(1):25–34. [PubMed: 24002178]
8. Woo SM, et al. Cell line IDG-SW3 replicates osteoblast-to-late-osteocyte differentiation in vitro and accelerates bone formation in vivo. J Bone Miner Res. 2011; 26(11):2634–46. [PubMed: 21735478]
9. Qing H, et al. Demonstration of osteocytic perilacunar/canalicular remodeling in mice during lactation. J Bone Miner Res. 2012; 27(5):1018–29. [PubMed: 22308018]
10. Stern AR, et al. Isolation and culture of primary osteocytes from the long bones of skeletally mature and aged mice. Biotechniques. 2012; 52(6):361–73. [PubMed: 22668415]
11. Kalajzic I, et al. Dentin matrix protein 1 expression during osteoblastic differentiation, generation of an osteocyte GFP-transgene. Bone. 2004; 35(1):74–82. [PubMed: 15207743]
12. Kern G, Flucher BE. Localization of transgenes and genotyping of H-2kb-tsA58 transgenic mice. Biotechniques. 2005; 38(1):38, 40, 42. [PubMed: 15679082]
13. D'Errico JA, et al. Employing a transgenic animal model to obtain cementoblasts in vitro. J Periodontol. 2000; 71(1):63–72. [PubMed: 10695940]
14. Kamel MA, et al. Activation of beta-catenin signaling in MLO-Y4 osteocytic cells versus 2T3 osteoblastic cells by fluid flow shear stress and PGE2: Implications for the study of mechanosensation in bone. Bone. 2010; 47(5):872–81. [PubMed: 20713195]
15. Cherian P, et al. Mechanical strain opens connexin 43 hemichannels in osteocytes: a novel mechanism for the release of prostaglandin. Mol Biol Cell. 2005; 16(7):3100–6. [PubMed: 15843434]
16. Kitase Y, et al. Mechanical induction of PGE(2) in osteocytes blocks glucocorticoid induced apoptosis through both the beta-catenin and PKA pathways. J Bone Miner Res. 2010

17. Boyan BD, et al. Localization of 1,25-(OH)2D3-responsive alkaline phosphatase in osteoblast-like cells (ROS 17/2.8, MG 63, and MC 3T3) and growth cartilage cells in culture. J Biol Chem. 1989; 264(20):11879–86. [PubMed: 2545688]
18. Barragan-Adjemian C, et al. Mechanism by which MLO-A5 late osteoblasts/early osteocytes mineralize in culture: similarities with mineralization of lamellar bone. Calcif Tissue Int. 2006; 79(5):340–53. [PubMed: 17115241]
19. Foster BL. Methods for studying tooth root cementum by light microscopy. Int J Oral Sci. 2012; 4(3):119–28. [PubMed: 22996273]
20. Winkler DG, et al. Osteocyte control of bone formation via sclerostin, a novel BMP antagonist. EMBO J. 2003; 22(23):6267–76. [PubMed: 14633986]
21. Jäger A, et al. Localization of SOST/sclerostin in cementocytes in vivo and in mineralizing periodontal ligament cells in vitro. J Periodontal Res. 2010; 45(2):246–54. [PubMed: 19778325]
22. Lehnen SD, et al. Immunohistochemical evidence for sclerostin during cementogenesis in mice. Ann Anat. 2012; 194(5):415–21. [PubMed: 22560000]
23. van Bezooijen R, et al. Sclerostin in mineralized matrices and van Buchem disease. J Dent Res. 2009; 88(6):569–74. [PubMed: 19587164]
24. Kuchler U, et al. Dental and periodontal phenotype in sclerostin knockout mice. Int J Oral Sci. 2014; 6(2):70–6. [PubMed: 24699186]
25. Schulze E, et al. Immunohistochemical investigations on the differentiation marker protein E11 in rat calvaria, calvaria cell culture and the osteoblastic cell line ROS 17/2.8. Histochem Cell Biol. 1999; 111(1):61–9. [PubMed: 9930885]
26. Wetterwald A, et al. Characterization and cloning of the E11 antigen, a marker expressed by rat osteoblasts and osteocytes. Bone. 1996; 18(2):125–32. [PubMed: 8833206]
27. Tenorio D, Cruchley A, Hughes F. Immunocytochemical investigation of the rat cementoblast phenotype. J Periodontal Res. 1993; 28(6 Pt 1):411–9. [PubMed: 8254458]
28. Schwab W, et al. Immunohistochemical localization of the differentiation marker E11 in dental development of rats. Acta Histochem. 1999; 101(4):431–6. [PubMed: 10611931]
29. Baba O, et al. Detection of dentin sialoprotein in rat periodontium. Eur J Oral Sci. 2004; 112(2): 163–70. [PubMed: 15056114]
30. Butler WT, et al. Nonocollagenous proteins of dentin. Isolation and partial characterization of rat dentin proteins and proteoglycans using a three-step preparative method. Coll Relat Res. 1981; 1(2):187–99. [PubMed: 6809409]
31. Suguro H, et al. Characterization of human dental pulp-derived cell lines. Int Endod J. 2008; 41(7): 609–16. [PubMed: 18479370]
32. Zhao S, et al. MLO-Y4 osteocyte-like cells support osteoclast formation and activation. J Bone Miner Res. 2002; 17(11):2068–79. [PubMed: 12412815]
33. Nakashima T, et al. Evidence for osteocyte regulation of bone homeostasis through RANKL expression. Nat Med. 2011; 17(10):1231–4. [PubMed: 21909105]
34. Ben-awadh AN, et al. Parathyroid hormone receptor signaling induces bone resorption in the adult skeleton by directly regulating the RANKL gene in osteocytes. Endocrinology. 2014; 155(8): 2797–809. [PubMed: 24877630]
35. Wijenayaka AR, et al. Sclerostin stimulates osteocyte support of osteoclast activity by a RANKL-dependent pathway. PLoS One. 2011; 6(10):e25900. [PubMed: 21991382]
36. Boabaid F, et al. The role of parathyroid hormone-related protein in the regulation of osteoclastogenesis by cementoblasts. J Periodontol. 2004; 75(9):1247–54. [PubMed: 15515341]
37. Galli C, Passeri G, Macaluso G. Osteocytes and WNT: the mechanical control of bone formation. J Dent Res. 2010; 89(4):331–43. [PubMed: 20200416]
38. Bonewald L, Johnson M. Osteocytes, mechanosensing and Wnt signaling. Bone. 2008; 42(4):606–15. [PubMed: 18280232]
39. Zhang K, et al. E11/gp38 selective expression in osteocytes: regulation by mechanical strain and role in dendrite elongation. Mol Cell Biol. 2006; 26(12):4539–52. [PubMed: 16738320]
40. Kagayama M, et al. Confocal microscopy of cementocytes and their lacunae and canaliculi in rat molars. Anat Embryol (Berl). 1997; 195(6):491–6. [PubMed: 9193723]

41. Scivetti M, et al. Confocal laser scanning microscopy of human cementocytes: analysis of three-dimensional image reconstruction. Ann Anat. 2007; 189(2):169–74. [PubMed: 17419549]
42. Suda R, et al. [Study of the penetration of extrinsic tracers into exposed cementum in vitro]. Nippon Shishubyo Gakkai Kaishi. 1989; 31(3):849–59. [PubMed: 2489533]
43. Ayasaka N, et al. Differences in the transport systems between cementocytes and osteocytes in rats using microperoxidase as a tracer. Arch Oral Biol. 1992; 37(5):363–9. [PubMed: 1610305]
44. Bosshardt D. Are cementoblasts a subpopulation of osteoblasts or a unique phenotype? J Dent Res. 2005; 84(5):390–406. [PubMed: 15840773]
45. Furseth R. A microradiographic and electron microscopic study of the cementum of human deciduous teeth. Acta Odontol Scand. 1967; 25(6):613–45. [PubMed: 5247243]
46. Jande S, Bélanger L. Fine structural study of rat molar cementum. Anat Rec. 1970; 167(4):439–63. [PubMed: 4195378]
47. Li X, et al. Targeted deletion of the sclerostin gene in mice results in increased bone formation and bone strength. J Bone Miner Res. 2008; 23(6):860–9. [PubMed: 18269310]
48. Thomas H. Root formation. Int J Dev Biol. 1995; 39(1):231–7. [PubMed: 7626411]
49. Walker CG, et al. Osteopontin is required for unloading-induced osteoclast recruitment and modulation of RANKL expression during tooth drift-associated bone remodeling, but not for super-eruption. Bone. 2010; 47(6):1020–9. [PubMed: 20828639]
50. Kagayama M, et al. Localization of uncalcified cementum in adult rat molar roots and its relation to physiological tooth movement. Arch Oral Biol. 1994; 39(10):829–32. [PubMed: 7741651]

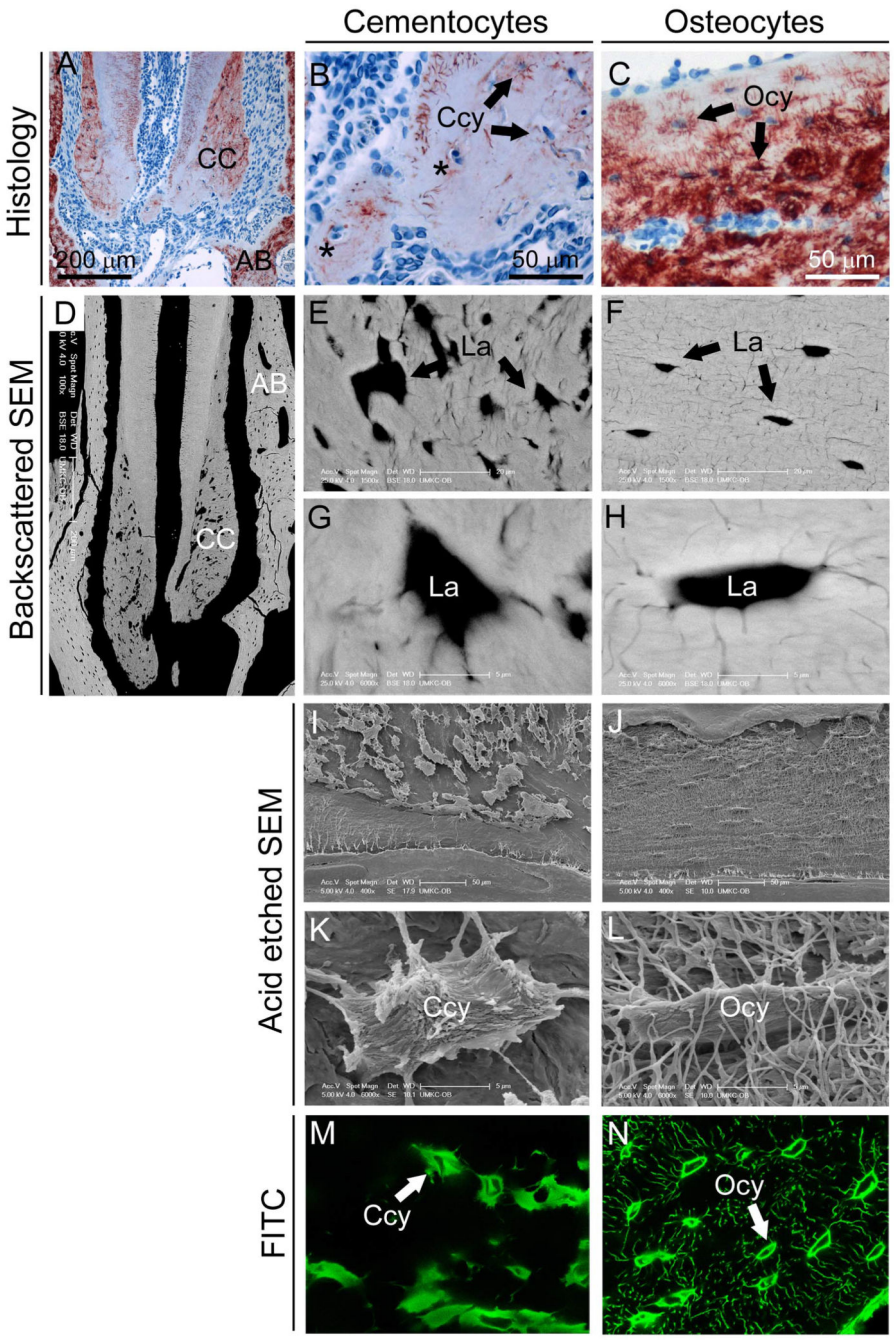

Figure 1. Differences in lacunar-canalicular network of cementocytes compared to osteocytes

(A) Histological examination of cellular cementum (CC) and surrounding alveolar bone (AB) of the first mandibular molar of a 2 month old mouse immunostained for dentin matrix protein 1 (DMP1). **(B)** Cellular cementum contains cementocytes (Ccy) occupying lacunae, as well as some lacunae containing more than one cell (black asterisks). **(C)** Alveolar bone includes numerous osteocytes (Ocy) within their lacunae. **(D)** Backscatter SEM showing cementocyte lacunae (La) in cellular cementum and osteocyte lacunae in alveolar bone. Compared to the regular spacing and ellipsoid shape of osteocyte lacunae **(E, G)**,

cementocyte lacunae exhibit irregular spacing and shape **(F, H)**. SEM of acid etched resin-embedded mandible allowed visualization of resin filled lacunae and revealing the **(I, K)** numerous canaliculi of osteocytes, whereas **(J, L)** cementocytes exhibited large, irregular lacunae with fewer canaliculi. These observations on the cementocytes canalicular network were confirmed using FITC staining **(M, N)**, where large and irregularly shaped cementocytes lacunae are surrounded by relatively few canaliculi.

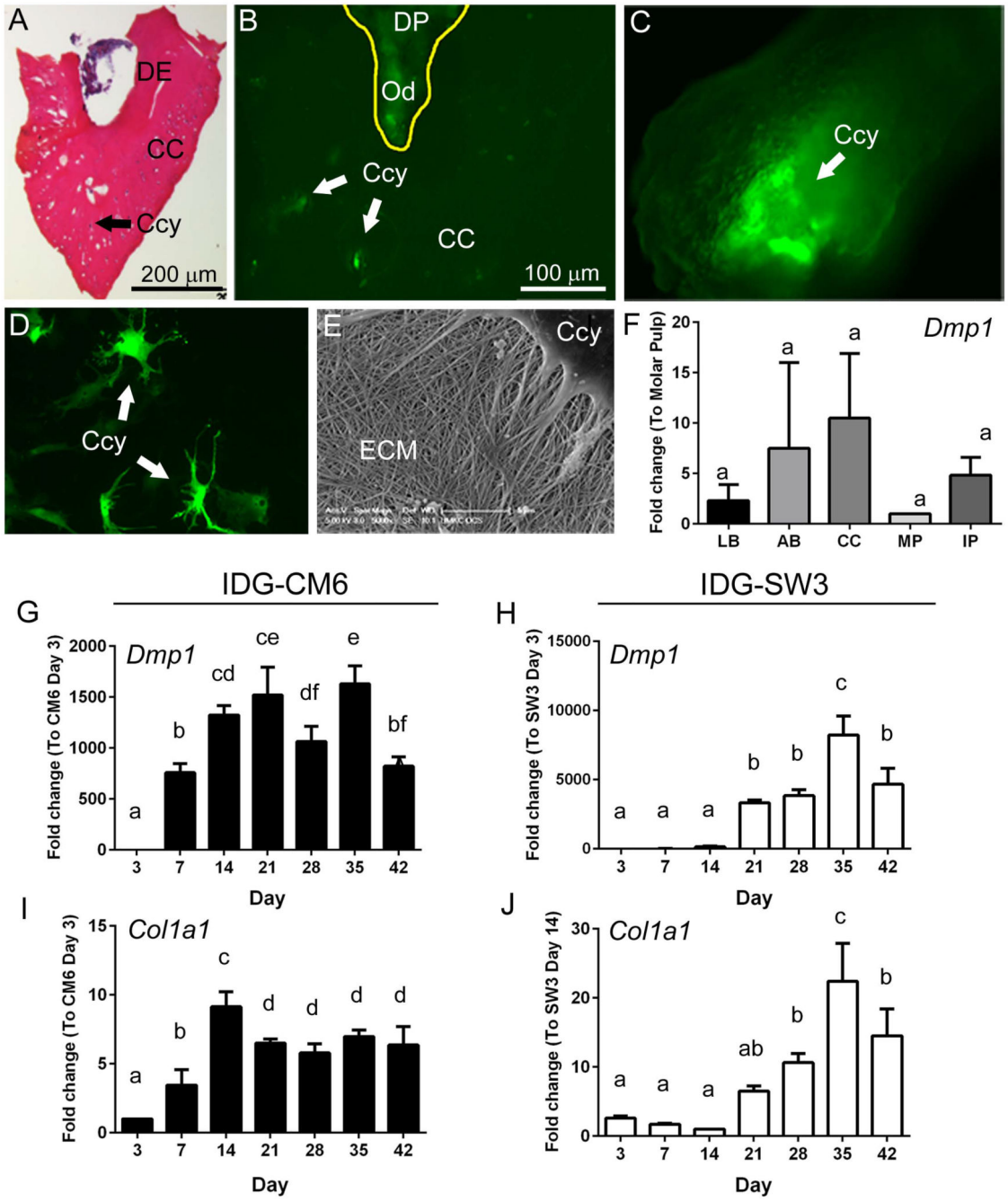

Figure 2. Isolation of DMP1-positive cementocytes and generation of the cell line IDG-CM6

(A) In order to isolate cementocytes (Ccy) from surrounding cells, molar teeth were extracted (excluding alveolar bone), and the apical portion of the molar root, including the dentin (DE) and cellular cementum (CC), was dissected, as shown in this H&E stained frozen tissue section. **(B)** DMP1 expressing (GFP-positive) cells in the apical tooth include cementocytes and odontoblasts (Od) within the dental pulp (DP). **(C)** During the enzymatic digestion to isolate cementocytes from the cementum matrix, GFP-positive are visible following digestion. After isolation, cloning, and 30 days in culture, IDG-CM6

cementocytes **(D)** maintain high DMP1 expression and exhibit the characteristic dendritic morphology. **(E)** SEM analysis of fixed IDG-CM6 cells after 14 days in culture confirmed production of an extracellular matrix (ECM) consistent with collagen. **(F)** Quantitative PCR analysis of total RNA isolated from fresh tissues indicates *Dmp1* expression in long bone (LB), alveolar bone, cellular cementum (CC), molar pulp (MP), and incisor pulp (IP) (n=4 for each tissue, the relative C_t values for Dmp1 were 23 – 29). No significant intergroup (tissue type) differences were detected by one-way ANOVA, as indicated by same lowercase letters above all bars. Quantitative PCR analysis over 42 days in culture indicates that **(G, H)** *Dmp1* and **(I, J)** *Col1a1* gene expression profiles are similar between IDG-CM6 cementocytes and IDG-SW3 osteocytes In G-J, data are presented as mean ± SD and IDG-CM6 and IDG-SW3 cells are graphed separately due to scale differences. (C_t values for IDG-CM6 Dmp1 were 18-31 and for Co1a1 were 12-16. IDG-SW3; Dmp1 23-36; Co1a1 14-18). One-way ANOVA and Tukey post-hoc test were used to indicate inter- or intragroup statistical significance. Different lowercase letters above bars indicate significant ($p < 0.05$) intragroup differences over time.

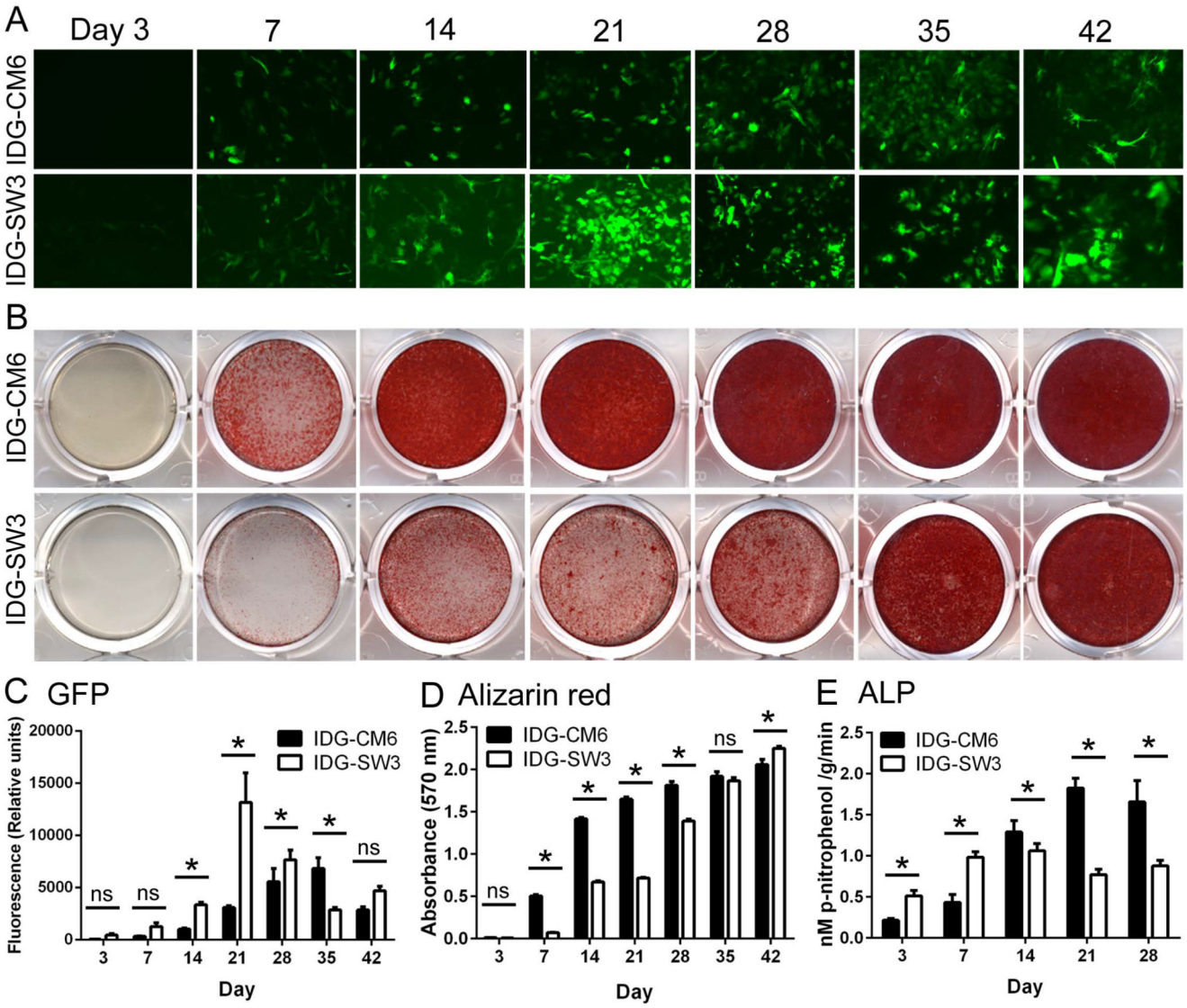

Figure 3. IDG-CM6 cementocytes mineralize in culture

IDG-CM6 cementocytes and IDG-SW3 osteocytes were cultured up to 42 days under mineralizing conditions (inclusion of 50 μg/ml ascorbic acid and 4 mM β-glycerophosphate). **(A, C)** *Dmp1*-driven GFP expression increases over time and shows a similar profile in IDG-CM6 and IDG-SW3 cells, however, cementocytes are slower to achieve peak GFP expression (day 35 vs. day 21 in IDG-SW3 cells). **(B, D)** By alizarin red staining, a detectable increase in mineral deposition by IDG-CM6 is observed by day 7, whereas IDG-SW3 cells initiate mineralization by day 14. Both cementocyte and osteocyte cultures became heavily mineralized over 42 days. **(E)** Alkaline phosphatase activity (ALP) activity increases in both cells over days 3-14, coincident with increased mineral deposition. In C-E, data are presented as mean ± SD. Two-way ANOVA and Bonferroni post-hoc test were used to indicate inter- and intragroup statistical significance, * $p < 0.05$; ns = not significant ($p > 0.05$).

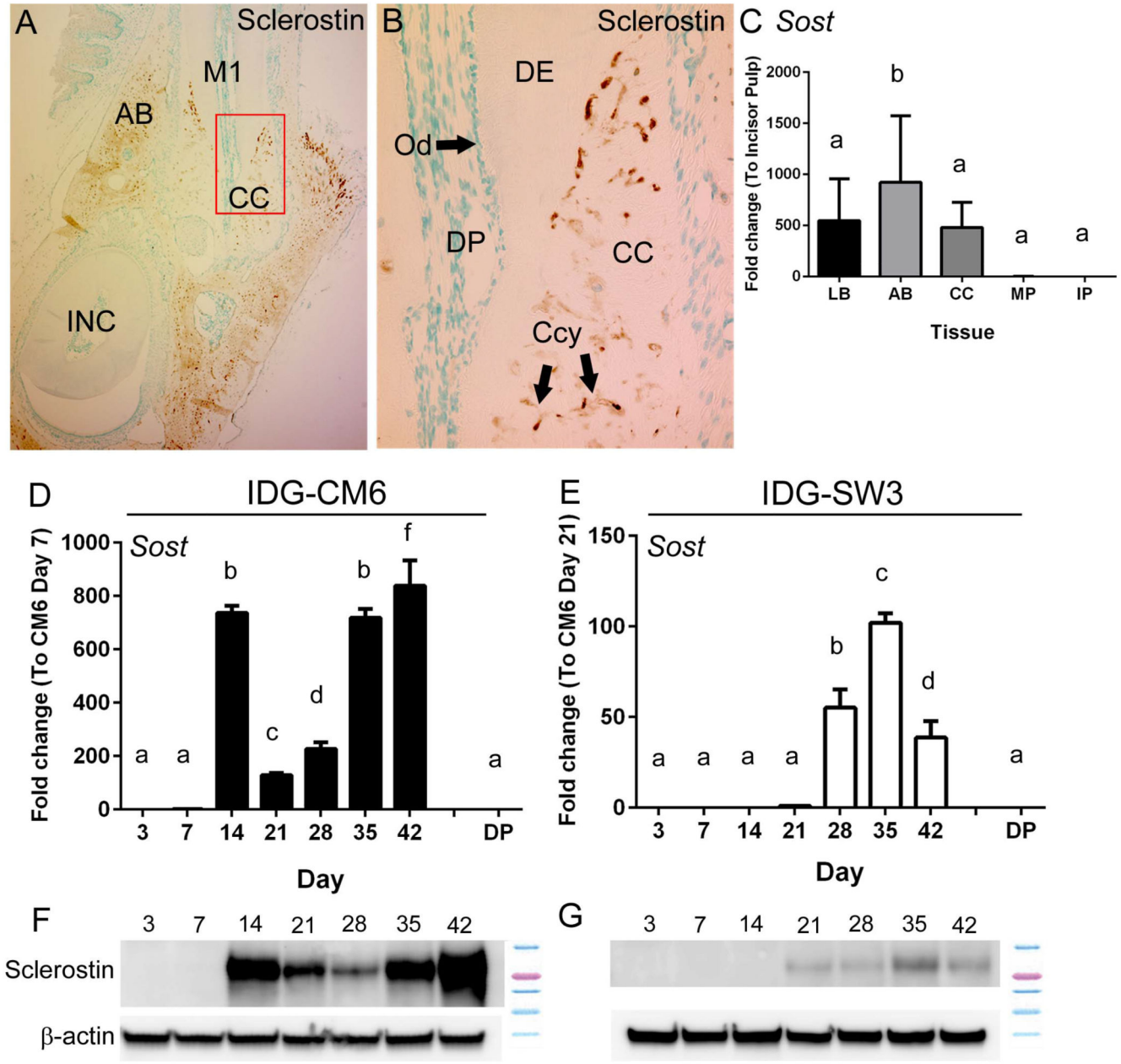

Figure 4. IDG-CM6 cementocytes express sclerostin

(A) Immunostaining for sclerostin in dentoalveolar tissues around the first molar (M1) of a 3 month old mouse shows localization in cellular cementum (CC) and alveolar bone (AB), but not in dental pulp or odontoblasts. Red box in panel A indicates region of higher magnification in panel B. **(B)** In cellular cementum, numerous cementocytes (Ccy) positive for sclerostin are observed. **(C)** Quantitative PCR from tissues confirms expression of *Sost* mRNA in long bone (LB), alveolar bone (AB), and cellular cementum (CC), but very low expression in molar and incisor pulp (MP and IP, respectively) (n=4 for each tissue, C_t values 23 – 36). IDG-CM6 cementocytes express **(D)** *Sost* mRNA and **(F)** sclerostin protein, in a biphasic profile with peaks at days 14 and 42. **(E)** IDG-SW3 cells express lower levels

of both **(E)** *Sost* mRNA and **(G)** sclerostin protein, and expression is not detected until approximately day 21. *Sost* mRNA expression from primary dental pulp (DP) is included in panels D and E as a reference for comparison to cells, *in vitro*. In C-E, data are presented as mean ± SD. In D and E, IDG-CM6 and IDG-SW3 cells are graphed separately due to scale differences. (C_t values for IDG-CM6: 22-33, IDG-SW3: 28-36). One-way ANOVA and Tukey post-hoc test were used to indicate inter- or intragroup statistical significance. Different lowercase letters above bars indicate significant ($p < 0.05$) intragroup differences over time.

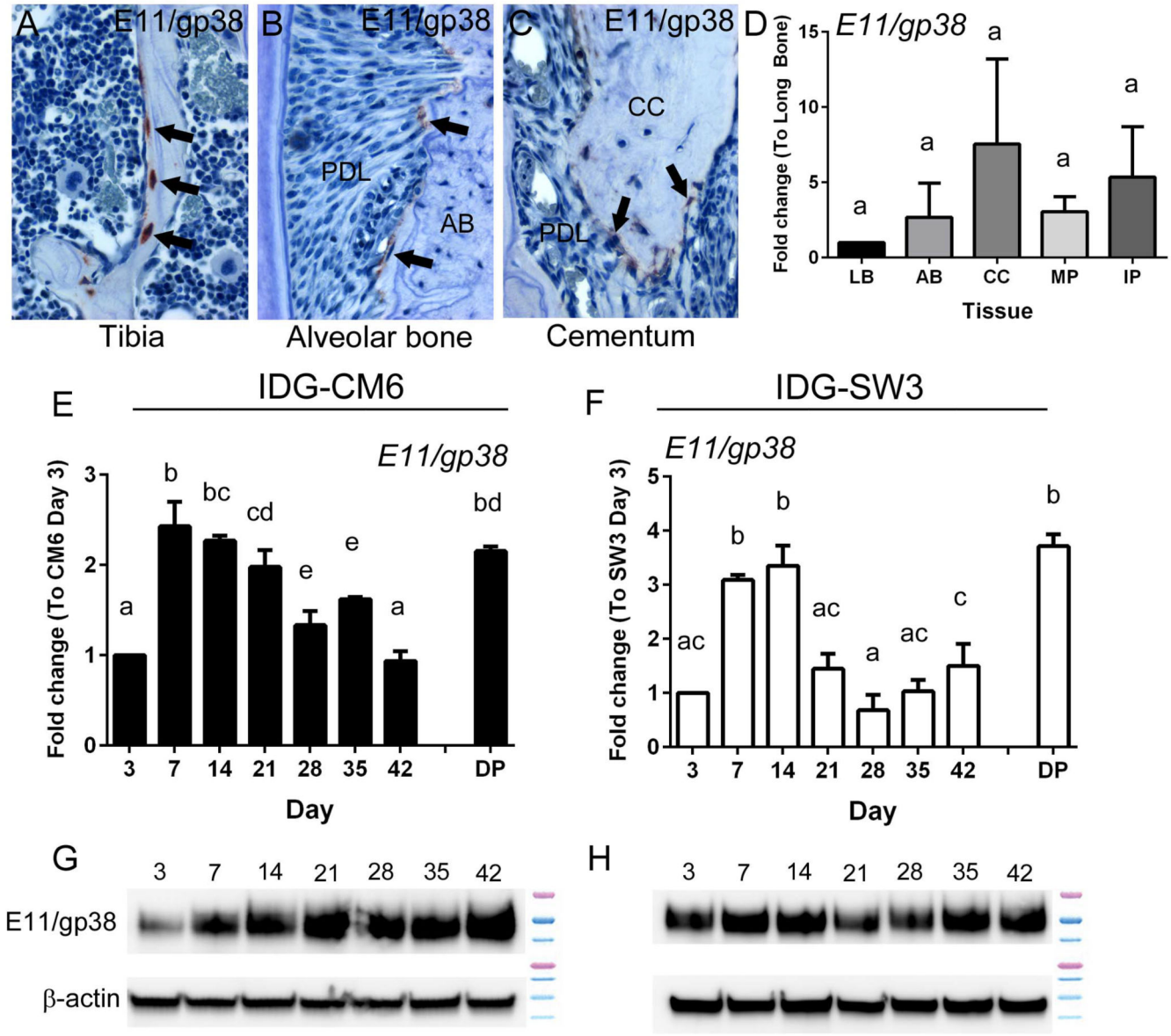

Figure 5. IDG-CM6 cementocytes express E11/gp38

Immunostaining for E11 in 3 month old mouse tissues shows localization in **(A)** new osteocytes in the tibia, with less expression in **(B)** new osteocytes of alveolar bone (AB) bordering the periodontal ligament (PDL), and **(C)** new cementocytes in cellular cementum (CC). Positively stained cells in panels A-C are indicated by black arrows. **(D)** Quantitative PCR from tissues confirms expression of *E11/gp38* mRNA in long bone (LB), alveolar bone (AB), cellular cementum (CC), and molar and incisor pulp (MP and IP, respectively) (n=4 for each tissue, Ct values 27 – 33). No significant intergroup differences were detected by one-way ANOVA, as indicated by same capital letters above tissue types. **(E-H)** Both IDG-CM6 and IDG-SW3 express E11/gp38 mRNA and protein over the course of 42 days in mineralizing media, *in vitro*. E11/gp38 mRNA expression from primary dental pulp (DP) is included in panels E and F as a reference for comparison to cells, *in vitro*. (C_t values for

IDG-CM6: 25-27, IDG-SW3: 24-29) In D-F, data are presented as mean ± SD. One-way ANOVA and Tukey post-hoc test were used to indicate inter- or intragroup statistical significance. Different lowercase letters above bars indicate significant ($p < 0.05$) intragroup differences over time.

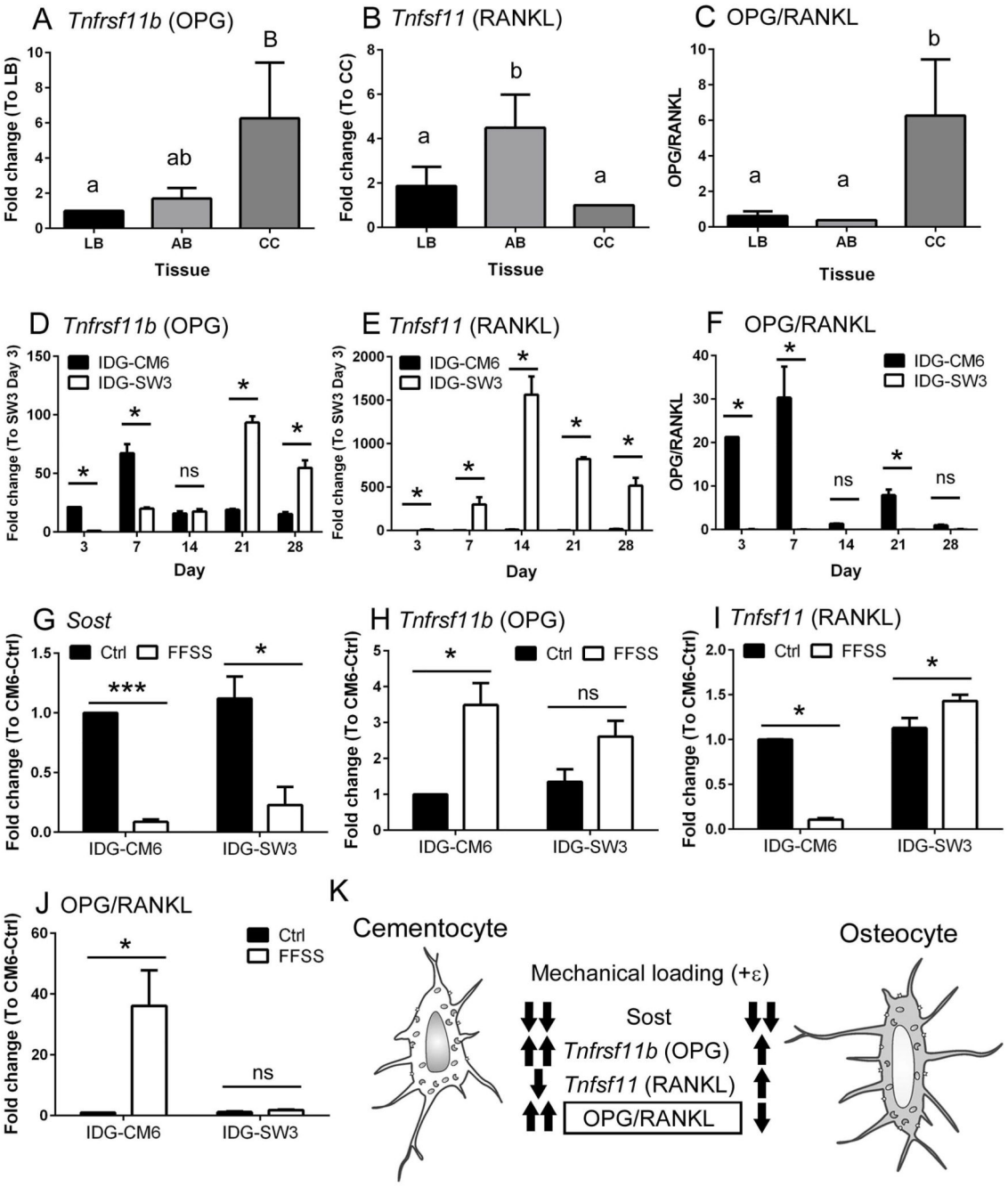

Figure 6. IDG-CM6 cells express OPG and RANKL and exhibit transcriptional changes in response to fluid flow shear stress

Quantitative PCR from tissues reveals **(A)** relatively high expression of *Tnfrsf11b* (gene for OPG) in cellular cementum (CC) versus long bone (LB) and alveolar bone (AB), **(B)** relatively low *Tnfsf11* (gene for RANKL), and **(C)** a significantly higher OPG/RANKL ratio in cementocytes vs. osteocytes from long bone or alveolar bone (n=4 for each tissue, C_t values for OPG 28 – 35 and for RANKL 28 – 37). **(D)** Over the course of 28 days in culture, IDG-CM6 cells express significantly higher *Tnfrsf11b* mRNA at some time points compared

to IDG-SW3 cells, peaking on day 7 and with no significant difference (ns) on day 14. (C_t values for IDG-CM6: 25-29, IDG-SW3: 26-35) **(E)** IDG-SW3 cells express considerably higher levels of *Tnfsf11* mRNA than do IDG-CM6 cells at all time points. (C_t values for IDG-CM6: 33-36, IDG-SW3: 26-32) **(F)** The relatively lower *Tnfsf11* expression in IDG-CM6 cells results in a significantly higher OPG/RANKL ratio compared to IDG-SW3 cells at days 3, 7, and 21. Fluid flow shear stress (FFSS) was used to analyze transcriptional changes in response to mechanical stimulus. IDG-CM6 and IDG-SW3 cells were grown for 21 days and then subjected to FFSS for 2 hrs at a setting of 8 dynes/cm^2. **(G)** *Sost* mRNA is significantly decreased by FFSS in both IDG-CM6 and IDG-SW3 cells. (C_t values for IDG-CM6: 22-33, IDG-SW3: 27-35) **(H)** FFSS stimulates a significant 4-fold increase in *Tnfrsf11b*/OPG in IDG-CM6 cells, while IDG-SW3 cells showed a non-significant trend in the same direction. (C_t values for IDG-CM6: 20-33, IDG-SW3: 26-26) **(I)** In response to FFSS, IDG-CM6 cells significantly decreased *Tnfsf11*/RANKL mRNA, whereas IDG-SW3 cells showed a significant increase. (C_t values for IDG-CM6: 34-37, IDG-SW3: 26-28) **(J)** IDG-CM6 cementocytes exhibit a statistically significantly 40-fold increased OPG/RANKL ratio, while IDG-SW3 osteocytes do not significantly alter their OPG/RANKL ratio suggesting. * indicates $p < 0.05$, *** indicates $p < 0.001$. **(K)** This model summarizes *in vitro* responses to mechanical stimulus (FFSS) of cementocytes (IDG-CM6) versus osteocytes (IDG-SW3). Whereas both cells decrease *Sost* mRNA in response to loading, cementocytes respond with greater *Tnfrsf11b*/OPG increase and significantly decreased *Tnfsf11*/RANKL, leading to a significantly increased OPG/RANKL ratio suggesting negative regulation of osteoclastogenesis. In A-J, data are presented as mean ± SD. In A-C, one-way ANOVA and Tukey post-hoc test were used to indicate statistical significance, where significant intergroup (tissue type) differences ($p < 0.05$) are indicated by different lower case letters above bars. In D-F, one-way ANOVA and Tukey post-hoc test were used to indicate statistical significance, where significant differences ($p < 0.05$) are indicated by * $p < 0.05$. In G-J, student t-test was used to indicate statistical significance, * $p < 0.05$; ** $p < 0.01$; *** $p < 0.001$.

Table 1

Procedure for isolation of IDG-CM6 cementocytes

Step 1	Mandibles were harvested (n=4), quickly rinsed in 70% ethanol, rinsed (2×) in water and kept in alpha-MEM (1% antibiotics (Pen/Strep) + 250 μg/mL gentamycin) at room temperature.
Step 2	1st and 3rd molars were extracted, and the apical portions of teeth were dissected and separated, and used for cementocyte isolation.
Step 3	Removal of PDL and pulp tissues from tooth root fragments was achieved by enzymatic digestion (300 U/mL type I collagenase for 30 minutes at 37°C), and supernatant was discarded.
Step 4	Tooth root fragments were subjected to (3×) serial digestions (collagenase A, 300 U/mL and EDTA, 5 mM/ 0.1% BSA, for 20 min each at 37°C), and the supernatant was discarded.
Step 5	Tooth fragments were rinsed with HBSS at 37°C (3-5×) and cultured in alpha-MEM added with 10% FBS and 1% antibiotics (Pen/Strep), 250 μg/mL gentamycin, and 50 U/mL IFN-γ at 33°C.
Step 6	Cell outgrowth was induced and monitored for GFP expression and a clone exhibiting GFP expression and mineralization was used for the subsequent studies.